Geophysica (1996), 32(1-2), 77-96

Prediction, Detection and Regional Assessment of Anthropogenic Climate Change

Ulrich Cubasch[1], *Gabriele C. Hegerl*[2] *and Jürgen Waszkewitz*[1]

1 DKRZ, Bundesstr. 55, D-20146 Hamburg, Germany

2 Max-Planck-Institut für Meteorologie, Bundesstr. 55, D-20146 Hamburg, Germany

(Received: August 1995; Accepted: July 1996)

Abstract

The paper reviews the present status of climate change modelling at the DKRZ and Max-Planck-Institute für Meteorologie in Hamburg. Increases in computing power have made it possible to run climate simulations which start already during the last century. This opens up a whole range of new options: the simulations can be compared with present day climate, the cold start error can be minimized and the climate change can already now be detected using a statistical fingerprint analysis. The inclusion of sulphate aerosols adds to the realism of the simulations.

In order to study the climate change in more detail, time-slice simulations with doubled horizontal resolution (T42) have been run. In this experimental technique the uncoupled atmosphere model is forced by the sea surface temperature and sea ice distribution calculated by the transient simulations with the coarse resolution globally coupled ocean-atmosphere model at the time of CO_2 doubling and tripling, and by the corresponding changed greenhouse gas concentration. It can be found with this technique, which simulates the changed climate under equilibrium conditions that the near surface temperature changes significantly, the precipitation, however, not significantly under future enhanced greenhouse gas conditions.

Key words: anthropogenic climate change, detection, time-slice experiments, sulphate aerosols

1. *Introduction*

Since the beginning of industrialization, the equivalent CO_2 content of the atmosphere has increased by 25 % and will have doubled by around the year 2035. Model simulations predict an anthropogenic climate change as a consequence of this accumulation of greenhouse gases (*IPCC*, 1990; 1992). An analysis of the model simulations revealed so far two major shortcomings of the experimental set-ups:

1. It has been shown by *Fichefet* and *Tricot* (1992) and *Hasselmann et al.* (1992), that it is important to take the warming since the beginning of the industrialization (ca. 1750) into account by using an earlier starting point for a climate change condition than present day conditions (typically 1980-1995). Experiments performed in Hamburg with a coupled ocean-atmosphere general circulation model (*CGCM; Cubasch et al.*, 1992, 1995a, b) prove the theoretical deductions about the neglect of the historic CO_2 effect and show that the initial conditions are of great importance for the estimate of the future climate. Furthermore it is now possible to compare the climate simulations with the observations for the historic time.

2. It only recently has become clear that the sulphate-aerosols play an important role in the present day climate and in the future climate. The effect of the sulphate-aerosols has firstly been simulated in a number of equilibrium simulations with mixed layer GCMs (*Roeckner et al.*, 1995; *Taylor* and *Penner*, 1994; *Santer et al.*, 1995), but now two model experiments with globally coupled ocean-atmosphere circulation models have been carried out in Hamburg and at the Hadley Centre in England with CGCMs (*Mitchell et al.*, 1995; *Hasselmann et al.*, 1995). The new set of experiments starting in historic time and taking into account the effect of sulphate aerosols will be discussed in Section 2.

There has been considerable scientific debate whether a statistically significant climate change - as predicted by the models - can already be detected in observed climate data (*Wigley* and *Raper*, 1990; *Barnett et al.*, 1991; *Santer et al.*, 1995). The measured increase in global mean near surface temperature of the order of 0.7°C since 1880 (*Jones* and *Briffa*, 1992) is consistent with the model predictions (*Cubasch et al.*, 1995a, *Mitchell et al.*, 1995). In Section 3, additional evidence for an anthropogenic climate change is added by applying an optimal fingerprint technique (*Hasselmann*, 1979; *Hasselmann*, 1993) to near surface temperature trends (*Hegerl et al.*, 1996). An attempt is made to quantify the probability that an anthropogenic climate signal can be detected in the observed temperature data and discern between different forcing scenarios.

A number of studies have been carried out to predict regional climate changes. These studies have attracted a lot of criticisms, since it was felt that the model resolution was too coarse and the model performance was too poor to allow for a regional interpretation of the results (*von Storch et al.*, 1993; *Grotch* and *McCracken*, 1991; *Wigley et al.*, 1990; *Karl et al.*, 1990; *Bardossy* and *Plate*, 1992). Various techniques are currently being employed to overcome this problem. Statistical downscaling methods (*Karl et al.*, 1990; *Bardossy* and *Plate*, 1992; *von Storch et al.*, 1993; *Zorita et al.*, 1995) derive and use an empiric statistical relationship between large-scale circulation patterns, which are reliably simulated by climate models, and regional climate and use this relationship for predicting regional climate change-assuming that the empirical relationship also holds for a changed climate. Dynamical regional high resolution models have been nested into global models (for an overview see: *Giorgi*, 1990; *Giorgi* and *Mearns*, 1991; *Mearns et al.*, 1995). These regional models have the advantage that affordable very high resolution simulations can be performed for a certain region of interest for a particular time, but have the disadvantage that they are currently coupled only one way, i.e. an interaction of the regional scale with the global scale is not possible. They therefore act only as a high resolution interpreter of the coarse information fed in at the boundaries. An alternative strategy using dynamical models is the so called "time slice" method using a global atmosphere model, which will be discussed in Section 4.

2. *Sulphate-aerosol experiments*

A set of simulations with the coupled atmosphere ocean model with a resolution of T21 has been started with the conditions of the year 1880 and has been continued up to the year 2050, twice with and once without the direct (albedo) effect of the sulphate-aerosols included (*Hasselmann et al.*, 1995; Fig. 1). All simulations were carried out using a new version of the Hamburg CGCM (i.e. ECHAM3 + LSG; for more details see *DKRZ*, 1994, *Cubasch et al.*, 1992; *Maier-Reimer et al.*, 1993; *Roeckner et al.*, 1992).

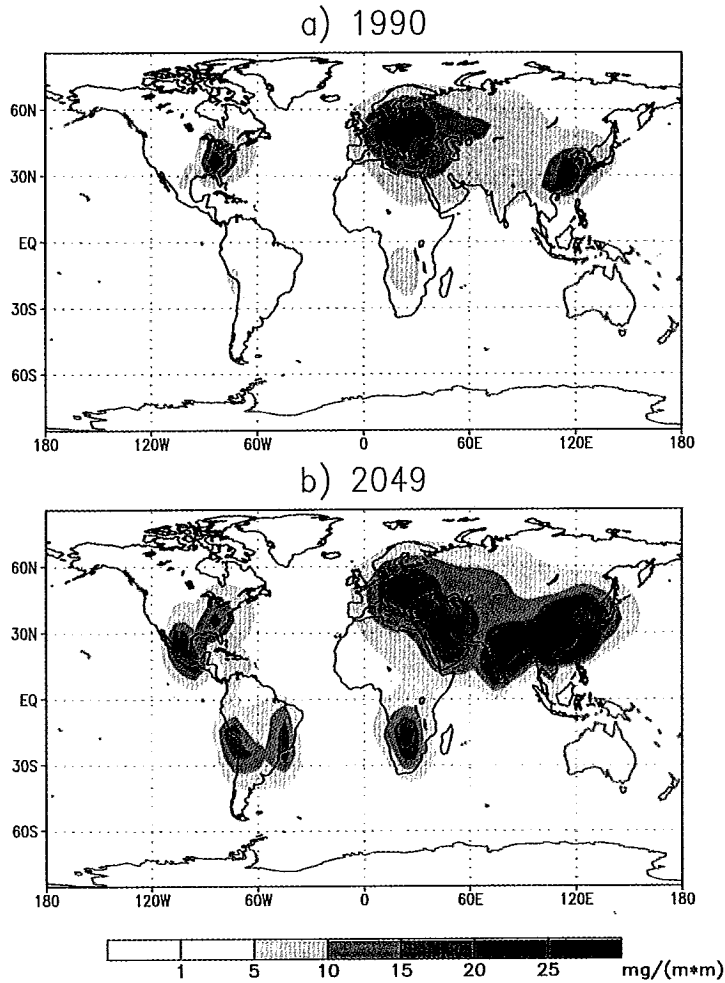

Fig. 1. The sulphate-aerosol loading for the decade 1981...1990 (top) and the decade 2040...2049 (bottom).

The aerosol data have been made available by the Meteorological Institute of the Stockholm University, they are based on observations until 1985 and on an IPCC scenario thereafter. The greenhouse gas forcing for the historic time up to now has been prescribed according to the observations, and for the future evolution the *IPCC* (1990) scenario A has been used. The sulphate-aerosol experiment has been run twice, both simulations differ only through the introduction of a small perturbation in the aerosol field in one of the runs. Using several simulations allows for a better separation of the climate change signal and the internal climate variability (represented by the independent fluctuations of the two simulations) in the model world.

The impact of the computed aerosol concentrations was represented in the CGCM as an increased effective surface albedo. Indirect effects of aerosols on the formation and radiative properties of clouds were not included. These are generally estimated to be of comparable magnitude to the direct effects, so that our computations of the aerosol climate impact must be regarded as only qualitative.

2.1 *Results of the aerosol-experiments*

Fig. 2 shows the time evolution of the globally averaged near surface temperature of the two aerosol experiments, the experiment without aerosols as well as the observations after *Jones* and *Briffa* (1992). The near surface temperature average has only been calculated in those gridboxes which have an adequate observational coverage. One can clearly see that the three curves run close together until about 1970. This means that the model is until that date quite capable to reproduce the observed temperature

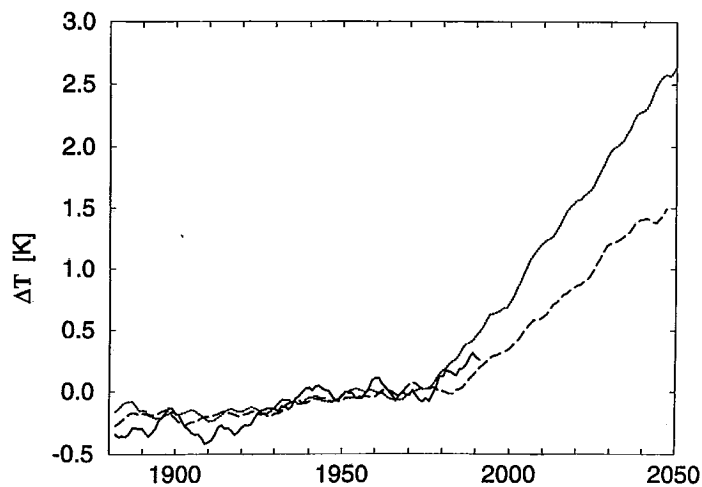

Fig. 2. The time evolution of the 5 year running mean near surface air temperature for the experiments with the CO_2 forcing only (dotted), for the mean of the aerosol experiments (dashed) and the observations (solid line). The x-axis describes the years, the y-axis the temperature change relative to the years 1951 to 1980. Only those points have been averaged for which a sufficient number of observations is available.

even without greenhouse gas increase or the aerosol effect. From 1975 onwards the CO_2 only experiment shows a temperature rise of about 0.3 K per decade, the aerosol experiments only ca. 0.2 K per decade. The curve of the observation appears to be closer to the curves of the aerosol experiment than to the CO_2 only experiment. The Hadley Center simulation (*Mitchell et al.*, 1995) obtains similar temperature increase rates with and without aerosol effect (*IPCC*, 1996).

Fig. 3 and Fig. 4 show the regional change of the near surface temperature for the experiments for the years 2040-2049 for summer and winter. The aerosols have a particularly large effect in the Northern hemisphere, since the main sources of the

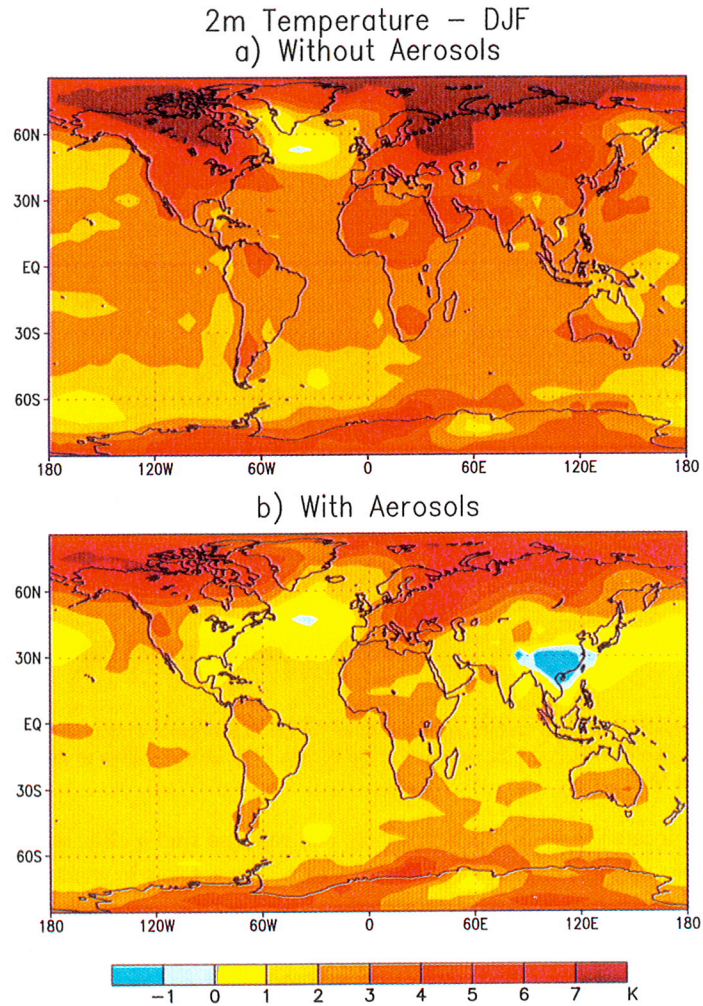

Fig. 3. The change of the near surface air temperature for the experiments without aerosol effect (top) and with aerosol effect (bottom) for winter for the decade 2040...2049 relative to the first decade of the experiment 1880...1889.

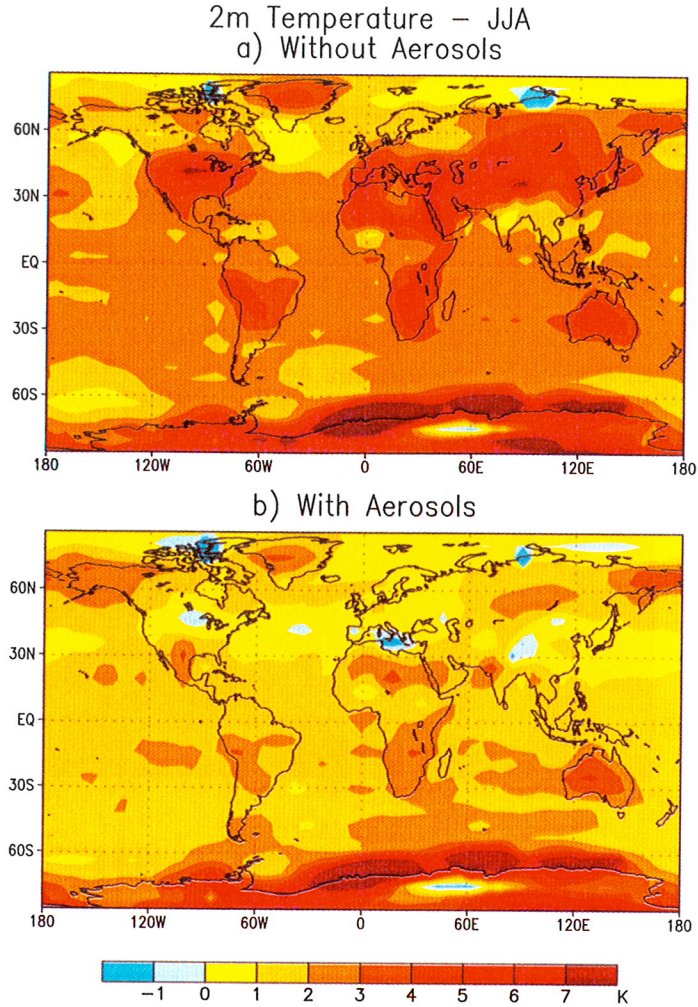

Fig. 4. The change of the near surface air temperature for the experiments without aerosol effect (top) and with aerosol effect (bottom) for summer for the decade 2040...2049 relative to the first decade of the experiment 1880...1889.

aerosols are located here. In this hemisphere one can also find a clear seasonal signal: in summer the aerosols have in most regions a larger impact than in winter, since due to the larger insolation their albedo effect is more effective. The impact of the aerosols on the Indian monsoon circulation is particularly remarkable. While without the aerosols most models predict a reinforcement of the monsoon (*IPCC*, 1992; 1996), the aerosol experiment indicate rather a decrease of the monsoon and the rainfall. This is caused by the local cooling over Central-East Asia caused by the aerosols, which damps the monsoon circulation (*Lal et al.*, 1995).

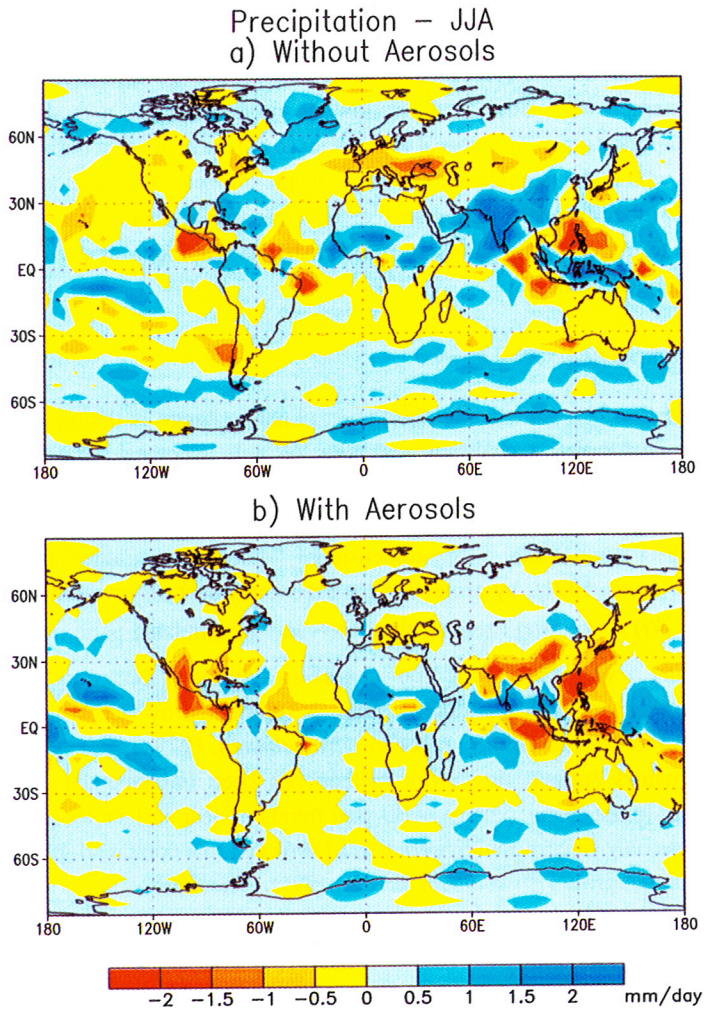

Fig. 5. The change of the precipitation for the experiments without aerosol effect (top) and with aerosol effect (bottom) for summer for the decade 2040...2049 relative to the first decade of the experiment 1880...1889.

3. *Detection of climate change*

The first step for proving (with a certain statistical confidence level) that the model-predicted climate change due to human activity can in fact be observed, is to investigate if the observations contain a significant climate change relative to the climate's "natural" variability. It has already been pointed out that estimates of natural climate variability are insufficient to explain the observed 100-year trend of global

mean temperature (e.g. *Stouffer et al.*, 1994, *Wigley* and *Raper* 1990). *Santer et al.* (1995) showed that there is an increasing trend in pattern correlation between a greenhouse gas and aerosol forced equilibrium climate change simulation and present near surface temperature data. In the following we demonstrate a method which is based on the application of an optimal fingerprint to derive a suitably defined detection variable for which the signal-to-noise ratio is maximized. This method allows to quantify the probability that the present climate change in near surface temperature trends is due to climate variability and to estimate the amplitude of a climate change signal from the observations.

3.1 The optimal fingerprint method

The question if a statistically significant climate change is taking place can be addressed by performing a statistical test with the null hypothesis that the observed warming is part of climate's natural variability. The model derived pattern of climate change (the "fingerprint") can be used as a statistical tool to condense the space-time dependent observations into a one-dimensional "detection variable" (*Hasselmann*, 1979; *Barnett et al.*, 1991), by projecting the time-dependent observations $\underline{\Psi}(t)$ on the fingerprint f, $d(t) = f^{1}\ \underline{\Psi}(t)$ (treating the observed and simulated patterns like vectors and performing a vector product). The idea of an optimized detection method is to modify the fingerprint such that climate noise is suppressed by weighting the model-derived pattern towards low-noise directions (*Hasselmann*, 1979; 1993).

Hasselmann's optimal fingerprint method has been implemented for detecting climate change in the spatial pattern of 30-year trends of near surface temperature for a greenhouse gas only fingerprint (*Hegerl et al.*, 1996) and to a combined greenhouse gas and aerosol fingerprint (*Hasselmann et al.*, 1995). The observations are based on instrumental data of near surface temperature from 1854 to 1994 (*Jones* and *Briffa*, 1992). The data are gridded by a 5° x 5° grid with increasing coverage over time. We rely upon the area covered regularly since 1949 (about 75 % of the globe). The fingerprint representing the expected pattern of near surface temperature trends due to anthropogenic climate change is taken from the mean of both combined greenhouse gas and aerosol simulations (c.f. Section 2). We use the dominant climate change pattern (i.e. first EOF) of the mean of both simulations, since we found that this pattern describes the increasing climate change pattern well (*Cubasch et al.*, 1992).

The noise estimate used for the optimization of the fingerprint is taken from a long "control" integration without external forcing (*von Storch*, 1994) with the ECHAM1/LSG CGCMs (which features an earlier version of the atmosphere model).

Fig. 6 shows the time evolution of the detection variable computed with running 30-year trend patterns from the observations. The recent rapid increase in the detection variable for the observations confirms the impression of Fig. 2 that the anthropogenic signal is now beginning to emerge from the natural variability noise.

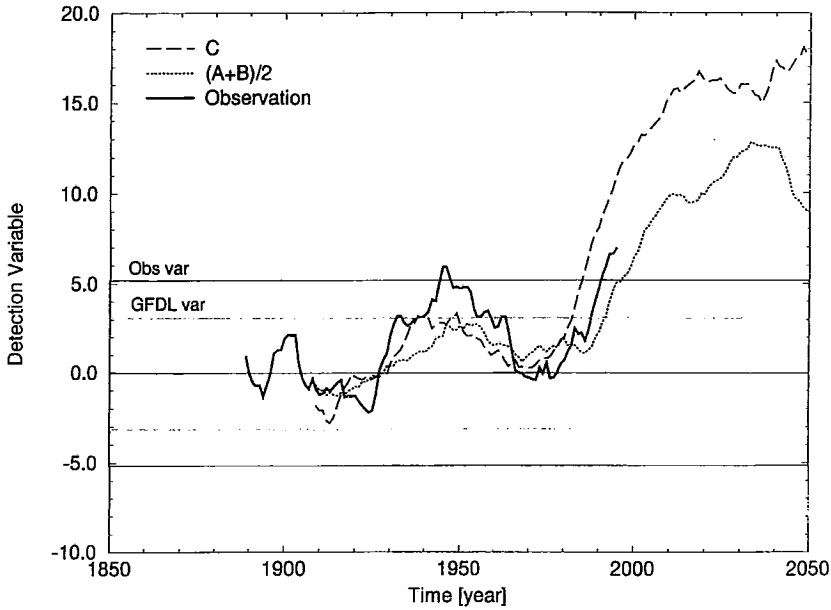

Fig. 6. Evolution of the detection variable using the optimal fingerprint for 30-year trend patterns computed from the observations (solid line), the mean of both combined forcing simulations (dotted line) and the greenhouse gas only simulation (dashed line). The time refers to the final year of the 30-year trend pattern (computed by a trend fitted to the time series of each gridpoint in each 30-year period). The 95 % confidence intervals derived from the observations (Obs var) and the GFDL control simulation (GFDL var) are indicated.

We formulate the null hypothesis that the latest observed trend pattern originates from natural climate variability. The information on the statistics of the detection variable for 30-year trend patterns is derived from observations (*Jones* and *Briffa*, 1992), after subtraction of a model derived estimate of the greenhouse warming signal (*Hegerl et al.*, 1996, and the GFDL CGCM control simulation over 1000 years (*Stouffer et al.*, 1994). The CGCM simulation used to estimate the covariance matrix C was excluded from the estimate, as this would have yielded an artificially suppressed value due to the non-independence of the data. Note that the model control simulations represent purely internal variability of the coupled climate system, disregarding naturally occurring forcing mechanisms such as volcanism or solar output variability. Thus, the ratio of the model-simulated to the observed variability as indicated by the confidence intervals of different width in Figure 6 appears not unreasonable. The estimate of the 95 % significance detection level from the variance of the time series for natural variability was corrected for sampling bias of the relatively short time series (especially in the case of the observations) by Monte Carlo simulations of a first-order auto-regressive process with the same autocorrelation time as the data (*Hegerl et al.*, 1996). Fig. 6 shows the 95 % confidence intervals derived by this procedure. Clearly, the latest observed trend is beyond this 95 % detection threshold.

Thus, the results indicate that the null-hypothesis is rejected, i.e. the recent temperature trends deviate from the model internal variability and also from observed variability with a risk of less than 5 % (2.5 % for a one-sided test taking into account that we expect positive values of the detection variable) and represent a significant climate change.

The detection variable has also been computed with data from both model simulations instead of the observations (Fig. 2), indicating what type of time evolution of the detection variable is expected from the model simulations. While the detection variable for the greenhouse gas forced simulation increases slightly before the observations, the mean of both aerosol and greenhouse gas forced simulations increases afterwards. Thus it is not possible to decide between the different forcing scenarios based on this figure.

Our significant results represent to a high degree the global mean temperature rise (see e.g. *Santer et al.*, 1994; *Hegerl et al.*, 1996). That the signal pattern structure after subtraction of the dominant global mean component nevertheless contributes to signal detection is demonstrated by Figure 7, which shows the spatial correlation (disregarding the global mean) between the observed trend data and the fingerprint from the combined forcing simulation on the one hand and from the greenhouse gas

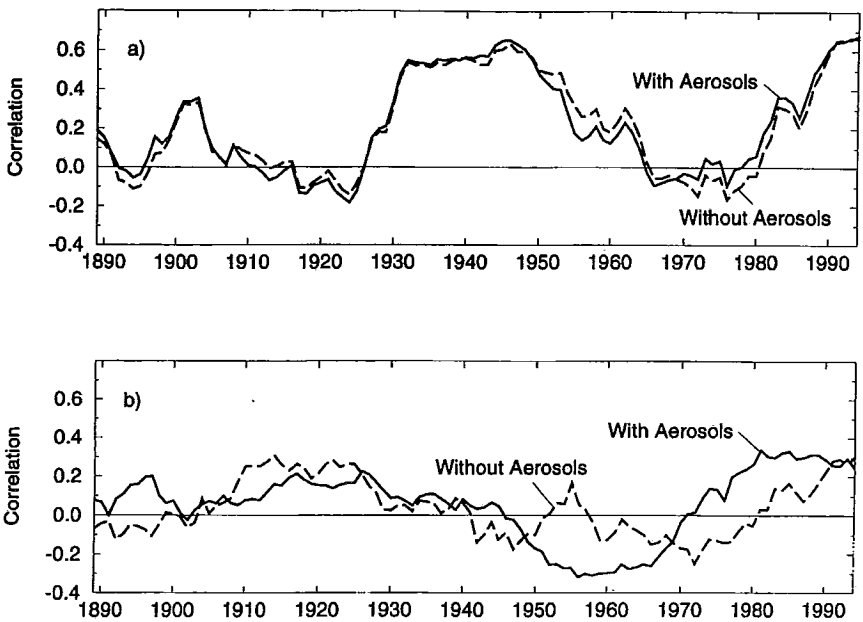

Fig. 7. Pattern correlations between observed 30 - year observed trends and the dominant climate change signal of the averaged equivalent CO_2 + aerosol simulations (full line) and for greenhouse-gas only simulation (equivalent CO_2 only; dashed line). In the top panel (a) the mean has not been removed, in the lower panel (b) the mean has been subtracted (after *Hasselmann et al.*, 1995).

only simulation (*Hasselmann et al.*, 1995) on the other hand. Both fingerprints are not optimized, since the optimal signal-to-noise ratio is only achieved if the mean value is included. The greenhouse gas only fingerprint is chosen as the dominant climate change signal for the respective simulation. For the 30-year trends ending between 1970 and 1990 the correlations are higher for the combined forcing fingerprint than for the greenhouse gas only fingerprint, in accordance with the findings of *Santer et al.* (1995). He also showed that the impact of aerosols which is strongest in the northern mid-latitudes in the summer, is seen more clearly if the data is seasonally stratified.

To make a more quantitative comparison between both fingerprints, we have projected the observations and model data synchronously onto the purely greenhouse gas induced fingerprint f_1 and onto a fingerprint f_2, which represents the additional component introduced by the combined forcing signal, i.e. which is orthogonal to the greenhouse gas only fingerprint and allows to compose the combined forcing fingerprint as a sum of f_1 and f_2. f_2 represents the hemispheric asymmetry introduced by the aerosol forcing: It shows warming in the southern hemisphere and cooling centered in the mid-latitude northern hemisphere where the strongest aerosol forcing occurs. Figure 8 shows that the observations generally have a positive contribution of the orthogonal fingerprint (represented by positive values on the vertical axes) after approximately the trend 1910-1940, indicating a component associated with the

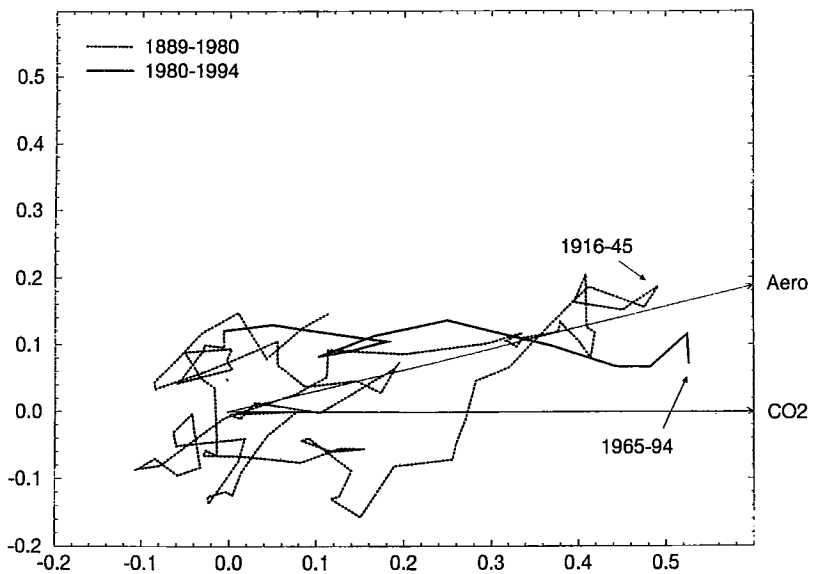

Fig. 8. Evolution of the observed temperature trends in a plane spanned by the (non-optimized) fingerprints for greenhouse gas and the orthogonal fingerprint which represents the hemispheric asymmetry introduced by the aerosol forcing. Both arrows indicate the greenhouse gas only (CO2) and the combined forcing fingerprint (Aero), which is not orthogonal to the greenhouse gas only fingerprint.

anthropogenic aerosol forcing. However, at present and with the present approach, both signals cannot be separated due to climate noise. However, if both fingerprints are optimized, the recent observed trend agrees substantially better with the combined forcing fingerprint (*Hegerl*, priv. comm.).

3.2 *Discussion of the detection analysis*

The most critical aspect of our analysis is clearly the estimate of the natural variability of the detection variable. Even though paleo-climatic data seem to suggest that the observed record of temperature represents rather strong variability in terms of 30-year trends, thus providing a conservative estimate, paleodata are not without problems. Therefore, when we want to assess whether the recent developments are "normal" or are reason for concern about the changes of the atmospheric composition, then we must assume that the instrumental record is good enough for estimating the basic statistics of climate variability, and that climate model and proxy data are good enough to further specify these statistics.

It is not automatically clear that this change has in fact been caused by the anthropogenic emissions. Other possible reasons of the climate change, e.g. changes in solar radiation, volcanic activity etc. have to be systematically excluded to rigorously attribute the observed warming to the anthropogenic forcing. This can be done e.g by using several fingerprints, as demonstrated above, and ruling out other possible forcing mechanisms.

4. *Time-slice experiments*

In this experimental technique the uncoupled atmosphere model is forced by the sea surface temperature (SST) and sea ice distribution is taken from a transient simulation[1] with a coarse resolution (T21, i.e. a Gaussian grid of 5.6^0) globally coupled ocean-atmosphere model (*Cubasch et al.*, 1992) at the point of CO_2 doubling ($2*CO_2$) and tripling ($3*CO_2$), and by the corresponding changed greenhouse gas concentration (*Mahfouf et al.*, 1994). All experiments, including a control simulation with present day climate conditions ($1*CO_2$) have been carried out with the ECHAM3 T42 model (T42, i.e. a Gaussian grid of 2.8^0) an integration time of 30 years and form therefore a kind of equilibrium experiments. A simulation of 5 years before the start of each simulation has been run to obtain the equilibrium and therefore is not used for the analysis. The model has been used in the AMIP model intercomparison (*Gleckler et al.*, 1994).

The time-slice method has the advantage that the model can be integrated for several decades around the time of interest with a high resolution, and that it gives a large statistical sample of the changed climate similar to equilibrium experiments with

[1] This experiment is an earlier experiment with an older model version than the one used for the aerosol-experiments. It has been started in the year 1985 and has therefore a substantial cold start error (*Cubasch et al.*, 1992).

mixed-layer models (see *IPCC*, 1990). Additionally it utilizes a more credible distribution of the SST than the mixed layer models.

4.1 Analysis of experiments

The model data are compared with the rainfall and surface temperature data after *Legates* and *Willmott* (1990a,b). Three of the six regions analyzed by *Cubasch et al.* (1995c) will be discussed in this particular report (Table 1). Only the changes on land points have been calculated. Two quantities are of primary concern for mankind and are among the most commonly measured, at least over land, i.e. precipitation and near surface temperature.

Table 1. The characteristics of the regions analysed.

No.	boundaries	location	number of land-gridpoints in area	areas defined according to
1	85° - 105° W, 35° - 50° N	Central North America	46	IPCC `90
2	70° - 105° E, 5° - 30° N	Southern Asia	69	IPCC `90
3	10° W - 45° E, 50° - 70° N	Central and Northern Europe	91	

4.2 Changes in surface temperature

The annual cycle of the surface temperature (Fig. 8) is simulated for Central North America in the 1*CO_2 simulation with the right amplitude, but with a warm bias of around 5 K in summer and winter. The temperature change is only marginal by going from 1*CO_2 to 2*CO_2 and exceeds only in the autumn and winter season 1 K. In the 3*CO_2 experiment, a clear signal is established with an average above 3 K. In this experiment the annual cycle is altered with a minimum change in spring and a maximum in late fall (longer Indian summer). The maximum in autumn is associated with an increased cloud cover, thus trapping the infrared radiation near the surface. In spring the cloud cover is reduced, allowing for more infrared cooling of the surface. The temperature changes for both, the 2*CO_2 and 3*CO_2 experiments, are significant. However, they are still smaller than the difference between the 1*CO_2 experiment and the observation. The year to year variability does not increase significantly in either experiment.

In Southern Asia the observed annual cycle of the near surface temperature is comparable with observations during spring and summer, but too cold during the other seasons (ca. 2 K in December). The temperature change for the 2*CO_2 experiment over Southern Asia is almost the same in every season, while in the 3*CO_2 simulation it has

a marked intraseasonal variability with a maximum of 4.5 K in March and a minimum of only 2 K in autumn. The temperature change is correlated with the change in the solar radiation at the top of the atmosphere with 0.74 and with the solar radiation reaching the surface with 0.77. The key to this phenomenon is the monsoon circulation. In March the conditions in this region are determined by flow from the North giving dry and clear sky conditions. In this case solar radiation passes almost unhindered to the surface, while the enhanced greenhouse effect directly warms the surface. During the pre-monsoon season (March) the radiative input at the surface is increased by up to 6 W/m^2 for the $3*CO_2$ simulation. In the summer, more and thicker clouds due to the enhanced hydrological cycle reflect more solar radiation at the top of the atmosphere and absorb more solar radiation on their way to the surface. During the summer month, an average of about 14 W/m^2 less solar radiation reaches the ground in the $3*CO_2$ simulation compared to the control simulation. Even though the thermal radiation is enhanced due to the greenhouse effect, the net radiation at the surface is reduced by about 2.5 W/m^2 during the summer month.

In Central and Northern Europe, the seasonal temperature cycle is simulated almost perfectly. In the $2*CO_2$ as well as in the $3*CO_2$ experiment the change of the temperature is significant and counteracts the seasonal cycle, i.e. the temperature change is much larger in winter than in summer, where in the $2*CO_2$ simulation only a moderate temperature change with a minimum in May and June can be found. In this simulation, only in the winter season the temperature change exceeds 1 K.

In some regions the temperature change is for both climate change simulations still smaller than the deviation of the simulation to observations. The predicted climate change for the $2*CO_2$ experiment generally only amounts to about 30 % to 40 % of the one obtained by the $3*CO_2$ experiment instead of the expected 50 %. This can be attributed to the cold start phenomenon (*Cubasch et al.*, 1995b; *Hasselmann et al.*, 1992). The $3*CO_2$ time-slice experiments resemble the CO_2 doubling equilibrium simulations with mixed-layer models (see *Schlesinger* and *Mitchell*, 1987) more than the $2*CO_2$ time-slice experiment (*Cubasch et al.*, 1995c).

4.3 Changes in precipitation

A thorough investigation of the hydrological cycle in the ECHAM3 model has been carried out by *Arpe et al.* (1994). It indicates that the uncertainties in the observations cause severe problems in the validation of the model results. The model simulates the precipitation mainly within the brackets of uncertainty of the observations. Instead of going through the exercise of comparing the model results to all available observations again, we restrict ourselves to the climatology of *Legates* and *Willmott* (1990a,b) bearing in mind the large uncertainty inherent in this dataset.

The simulated precipitation over Central North America completely misses the peak in late spring and early summer (Fig. 9). The mean value is only about 50 % of the observed amount. The precipitation does not significantly change in Central North

America in any of the climate change simulations. Differences of a maximum of 20 % still fall within the interannual variability of the control simulation. The interannual variability is not significantly altered either.

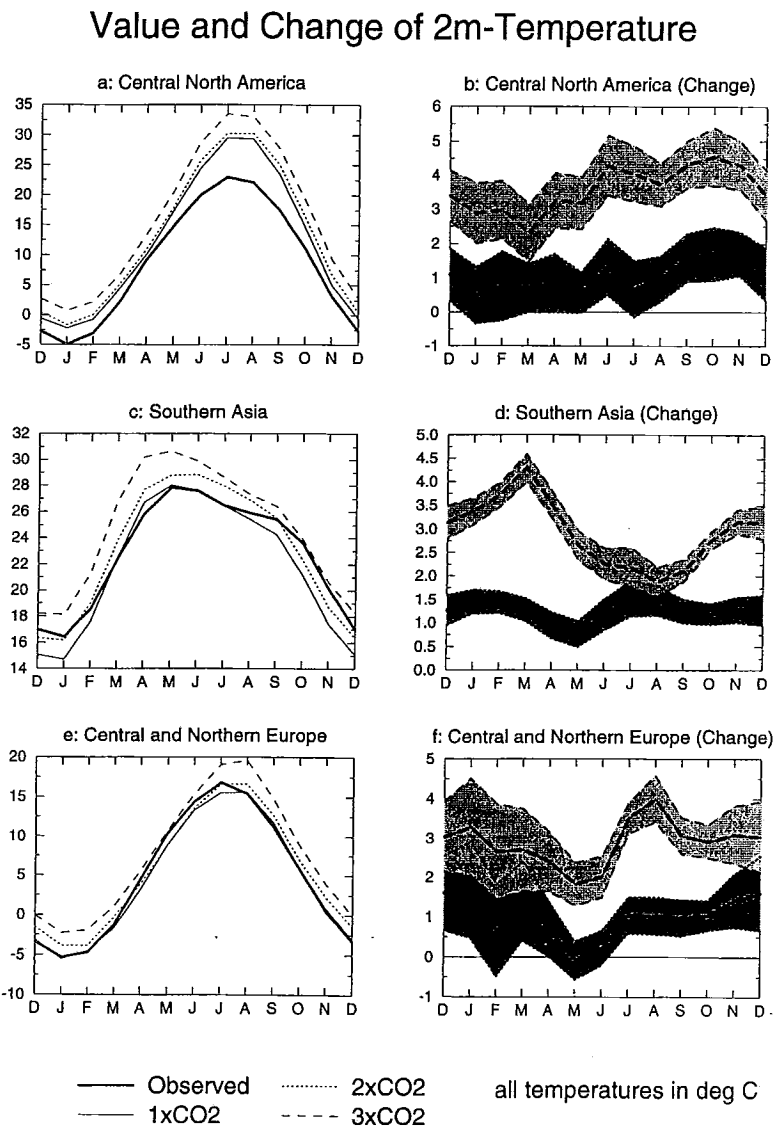

Fig. 9. The annual cycle of the near surface temperature [°C] (panels a, c and e) and its change (panels b, d and f) for the 2*CO_2 (dotted) and 3*CO_2 (dashed) integrations for Central North America (a) Southern Asia (b), and Central and Northern Europe (c). The observation have been drawn with bold solid lines, the 1*CO_2 experiment with thin solid lines. The shading surrounding the change curves indicates the 95 % significance limits (after *Cubasch et al.*, 1995c).

The precipitation over Southern Asia has a marked seasonal cycle with a minimum in early spring (the winter monsoon) and a maximum in late summer. The annual cycle of precipitation is simulated quite well over Southern Asia, even though the maximum during the summer monsoon season is underestimated about 30 %. This, of course, also drags the mean simulated value below the observed mean.

Under the $2*CO_2$ conditions this situation is hardly altered, and changes are barely significant. Under the $3*CO_2$ conditions, the precipitation in the monsoon season increases by 10 %. It has already been stressed by *Lal et al.* (1995) that the enhanced hydrological cycle results in an increase of the monsoon precipitation over India. The interannual variability is not significantly influenced by the greenhouse gas concentration. This statement, however holds only for those simulations, where the direct sulphate aerosol effect has not been taken into account (c.f. Section 2).

The observed summer precipitation of Central and Northern Europe shows a relative maximum while the model simulates a minimum. During the other seasons the observed and simulated values agree quite well. The mean value is underestimated. Under climate change conditions, the model predicts on average a drying, which reaches its maximum during the (already unreasonably dry) summer season, but which is not statistically significant. This decrease of precipitation is slightly higher in the $3*CO_2$ compared to the $2*CO_2$ experiment.

The analysis of the seasonal precipitation shows that this parameter is only poorly simulated. The change of precipitation confirms the statements made by *Santer et al.* (1994) that precipitation has a low signal-to-noise ratio, because it does not show an unequivocal sign. Even the tripling of CO_2, which has a large impact on the near surface temperature, did not influence precipitation in a distinct way, with the exception of Southern Asia and the Sahel. Generally the deviation in the precipitation simulation compared to observations is larger than the predicted climate change.

5. *Summary and conclusions*

The inclusion of sulphate aerosols and the early start of the simulation at the end of the last century create a realistic simulation of the present day climate. For the future climate the aerosol effect causes a local cooling over some parts of the northern hemisphere, particularly in summer.

Using model predictions of anthropogenic climate change in an optimal fingerprint method, it can be tentatively concluded that the probability that the observed temperature increase during the last decades is of natural origin is less than 5 %, i.e. that the observed global warming is very likely due to man's activities. The estimate of natural variability of climate has been assessed by the observations (with an estimated greenhouse warming signal subtracted), and by two 1000-year CGCM simulations of the present climate (*von Storch*, 1994; *Stouffer et al.*, 1994). The fact that the recent warming coincides closely with the increased greenhouse warming predicted by coupled ocean-atmosphere general circulation models as well as the agreement between

the pattern of the combined forcing fingerprint and the observations is strong circumstantial evidence that the observed temperature change is indeed anthropogenic.

The time-slice method provides a mean to assess the regional climate change with higher resolution and with a statistical sufficient sample, because it operates at an equilibrium state. The temperature changes regionally significantly at doubling and tripling of the atmospheric CO_2 concentrations, while the precipitation changes are less clear determined and statistically not significant. It has to be stressed that the time-slice experiments do not yet take the direct effect of aerosols into consideration, not because this effect is not important but because they have been based on a set of earlier experiments.

Furthermore, the inclusion of aerosols can change the sign of the precipitation change over certain regions of the globe. This indicates how sensitive regional precipitation change is to the specification of the anthropogenic forcing (whose magnitude, in the case of the sulfate aerosol forcing, is highly uncertain).

6. *Outlook*

Despite all the effort it cannot be excluded that important parameters or experimental conditions have not yet been included or that apparently negligible parameters become important in a climate change simulation. The sensitivity of the results to the inclusion of just one effect of the sulphate aerosols, or the starting date of the integration are indicating it. From the modelers side obvious shortcomings will be dealt with and new ideas will be implemented as they emerge. Plans have been drawn up to calculate directly from the sulphate aerosol emissions and their transport the direct effect interactively. Plan have been made to include the indirect aerosol effect at a later stage as well.

As the horizontal resolution is a major problem, it is planned to carry out the transient simulations with a T42 model and the time slice experiments with a T106 model.

Acknowledgments

The author expresses his thanks to K. Hasselmann, L. Bengtsson and E. Roeckner for the scientific support of this project. The simulations have been sponsored by the "Ministerium für Bildung, Wissenschaft, Forschung und Technologie", the "Max-Planck-Gesellschaft" as well as by the European Commission (EV5V-CT92-0123). The aerosol-data have been provided by the Meteorological Institute of the Stockholm University. The calculations have been carried out at the DKRZ by R. Voss and A. Hellbach.

7. *References*

Arpe, K., L. Bengtsson, L. Dümenil and E. Roeckner, 1994. The hydrological cycle in the ECHAM3 simulations of the atmospheric circulation. In: *Global precipitation and climate change*, Eds: Desbois, M. and F. Desalmond, NATO ASI Series, Vol I, **26**, 361-377.

Bardossy, A. and E.J. Plate, 1992. Space-time models for daily rainfall using atmospheric circulation patters. *Water Resource Res., 28, 1247-1259.*

Barnett, T.P., H. Ellsaesser, P. Ya. Groisman , S. Grotch, G. Jenkins, D. Karoly, M. Riches, B.D. Santer, C.D. Schönwiese, F. Vinnikov and F. Zwiers, 1991. Greenhouse signal detection. In: Greenhouse-Gas-InducedClimatic Change: A Critical Appraisal of Simulations and Observations, (Schlesinger M.E. ed.). 593-602. Elsevier Science Publishers, Amsterdam.

Cubasch, U., K. Hasselmann, H. Höck, E. Maier-Reimer, U. Mikolajewicz, B.D. Santer, and R. Sausen, 1992. Time-dependent greenhouse warming computations with a coupled ocean-atmosphere model. *Climate Dynamics*, **8**, 55-69.

Cubasch, U., B.D. Santer, A. Hellbach, G. Hegerl, H. Höck, E. Maier-Reimer, U. Mikolajewicz, A. Stössel, and R. Voss, 1994. Monte Carlo climate change forecasts with a global coupled ocean-atmosphere model. *Climate Dynamics*, **10**, 1-19.

Cubasch, U., B.D. Santer and G. Hegerl, 1995a. Klimamodelle - wo stehen wir? *Phys. Bl.*, **51**, 269-276.

Cubasch, U., G. Hegerl, A. Hellbach, H. Höck, U. Mikolajewicz, B.D. Santer and R. Voss, 1995b. A climate change simulation starting 1935. *Climate Dynamics*, **11**, 71-84.

Cubasch, U., J. Waszkewitz, G. Hegerl and J. Perlwitz, 1995c. Regional climate changes as simulated in time-slice experiments. *Climatic Change*, **31**, 273-304.

DKRZ, 1994. The ECHAM3 atmospheric general circulation model. Techn. Rep. No. 6, Deutsches Klimarechenzentrum, Hamburg, Germany.

Fichefet, T. and C. Tricot, 1992. Influence of the starting date of model integration on projections of greenhouse-gas-induced climatic change. *Geophys Res. Lett.* **19**, 1771-1774.

Giorgi, F., 1990. Simulations of regional climate using limited-models nested in a general circulation models. *J. Climate* **3**, 941-963.

Giorgi, F. and L. Mearns, 1991. Approaches to the simulation of regional climate change: A review. *J. Geophys. Res.*, **29**, 191-216.

Gleckler, P.J., D.A. Randall, G. Boer, R. Colmann, M. Dix, V. Galin, M. Helfand, J. Kiehl, A. Kitoh, W. Lau, XZ Liang, V. Lykossov, B. McAvaney, K. Miyakoda, S. Planton, 1994. Cloud-radiative effects on implied oceanic energy transports as simulated by atmospheric general circulation models. PCMDI Report No. 15, PCMDI/LLNL, Livermore, Ca., USA.

Grotch, S.L. and M.C. MacCracken, 1991. The use of general circulation models to predict regional climate change. *J. Climate* **4**, 286-303.

Hasselmann, K., R. Sausen, E. Maier-Reimer and R. Voss, 1992. On the cold start problem in transient simulations with coupled ocean-atmosphere models. *Climate Dynamics*, **9**, 53-61.

Hasselmann, K., 1979. On the signal-to-noise problem in atmospheric response studies. In: Meteorology of Tropical Oceans. Royal Meteorological Society, 251-259.

Hasselmann, K., 1993. Optimal fingerprints for the detection of time dependent climate change. *J. Climate*, **6**, 1957-1971.

Hasselmann K., L. Bengtsson, U. Cubasch, G.C. Hegerl, H. Rodhe, E. Roeckner, H. von Storch, R. Voss, and J. Waszkewitz, 1995. Detection of anthropogenic climate change using a fingerprint method. MPI report, 168.

Hegerl, G.C., H. von Storch, K. Hasselmann, B.D. Santer, U. Cubasch and P.D. Jones, 1996. Detecting anthropogenic climate change with an optimal fingerprint method. *J. Climate*, in press.

IPCC, 1990. Climate change: The IPCC scientific assessment. Eds. Hougthon., G.J. Jenkins, and J.J. Ephraums. Cambridge University Press, Cambridge, 364 pp.

IPCC, 1992. Climate change: The supplementary report to the IPCC scientific assessment. Eds. J. Houghton, B. A. Callendar and S. K. Varney, Cambridge University Press, 198 pp.

IPCC, 1996. Climate change 1995 - The science of climate change: Eds. J. Houghton, L. Meira Filho, B.A. Callendar, N. Harris, A. Kattenberg and K. Maskell, Cambridge University Press, 572 pp. 1996.

Jones, P.D., and K.R. Briffa, 1992. Global surface air temperature variations during the twenties century: Part 1, spatial, temporal and seasonal details. *The Holocene*, **2**, 165-179.

Karl, T.R., W.-C. Wang, M.E. Schlesinger and R.W. Knight, 1990. A method of relating general circulation model simulated climate to the observed local climate, Part I: Seasonal statistics. *J. Climate*, **3**, 1053-1079.

Lal, M., U. Cubasch, R. Voss and J. Waszkewitz, 1995. The transient response of greenhouse gases and sulphate aerosols on monsoon climate. *Current Science*, **69**, 752-762.

Legates, D.R. and C.J. Willmott, 1990a. Mean seasonal and spatial variability in gauge corrected global surface air temperature. *J. Climatology*, **41**, 11-21.

Legates, D.R. and C.J. Willmott, 1990b. Mean seasonal and spatial variability in gauge corrected global precipitation. *J. Climatology*, **10**, 111-127.

Mahfouf, J.F., D. Cariolle, J.-F. Royer, J.-F. Geleyn and B. Timbal, 1994. Responses of the Meteo-France climate model to changes in CO_2 and sea surface temperature. *Climate Dynamics*, **9**, 345-362.

Maier-Reimer, E., U. Mikolajewicz and K. Hasselmann, 1993. Mean circulation of the Hamburg LSG OGCM and its sensitivity to the thermohaline surface forcing. *J. Phys. Oceanography*, **23**, 731-757.

Mearns, L.O., F. Giorgi, M. McDaniel and C. Shields, 1995. Analysis of daily variability of precipitation in a nested regional climate model: comparison with observations and doubled CO_2 results. *Global Planet. Change* **10**, 55-78.

Mitchell, J.F.B., T.C. Johns, J.M. Gregory and S.F.B. Tett, 1995. Climate response to increasing levels of greenhouse gases and sulphate aerosols. *Nature*, **376**, 501-504.

Roeckner, E., K. Arpe, L. Bengtsson, S Brinkop, L. Dümenil, M. Esch, E. Kirk, F. Lunkeit, M. Ponater, B. Rockel, R. Sausen, U. Schlese, S. Schubert and M. Windelband, 1992. Simulation of the present-day climate with the ECHAM model: impact of model physics and resolution. Report No. 93, Max-Planck-Institut für Meteorologie, Bundestr. 55, Hamburg, Germany.

Roeckner, E., T. Siebert and J. Feichter, 1995. Climatic response to anthropogenic sulfate forcing simulated with a general circulation model. In: Aerosol forcing of climate, Charlson, R. J., and J. Heintzenberg (Eds), J. Wiley & Sons, 1995.

Santer B.D., W. Brüggemann, U. Cubasch, K. Hasselmann, E. Maier-Reimer and U. Mikolajewicz, 1994. Signal-to-noise analysis of time-dependent greenhouse warming experiments. Part 1: Pattern analysis. *Climate Dynamics*, **9**, 267-285.

Santer B.D., K.E. Taylor, J.E. Penner, T.M.L. Wigley, P.D. Jones and U. Cubasch, 1995. Towards the detection and attribution of an anthropogenic effect on climate. *Climate Dynamics*, **12**, 77-100.

Stouffer, R.J., S. Manabe, and K.Y. Vinnikov, 1994. Model assessment of the role of natural variability in recent global warming. *Nature*, **367**, 634-636.

von Storch, H., E. Zorita and U. Cubasch, 1993. Downscaling of climate change estimates to regional scales: application to winter rainfall in the Iberian Peninsula. *J. Climate* **6**, 1161-1171.

Taylor, K., and J. Penner, 1994. Climate system response to aerosols and greenhouse gases: a model study. *Nature*, **369**, 734-737.

Wigley, T.M.L., and S.C.B. Raper, 1990. Natural variability of the climate system and detection of the greenhouse effect. *Nature*, **344**, 324-327.

Wigley, T.M.L., P.D. Jones, K.R. Briffa, and G. Smith, 1990. Obtaining subgrid scale information from coarse-resolution general circulation model output. *J. Geophys. Res.*, **95**, 1943-1953.

Zorita, E., J. Hughes, D. Lettenmaier, and H. von Storch, 1995. Stochastic characterisation of regional circulation patterns for climate model diagnosis and estimation of local precipitation. *J. Climate*, **8**, 1023-1042.